

Electrolytic preparation of CaB_6 by molten salt technique

S. Angappan · M. Helan · A. Visuvasam ·
L. John Berchmans · V. Ananth

Received: 15 October 2009 / Revised: 19 January 2011 / Accepted: 13 February 2011 / Published online: 16 March 2011
© Springer-Verlag 2011

Abstract Calcium hexaboride (CaB_6) crystals with high melting point (2,235 °C) have been conveniently synthesized at low temperature (900 °C) from molten salt electrolysis. The synthesis was carried out using $\text{CaO-B}_2\text{O}_3\text{-LiF}$ melt under argon atmosphere. Electrochemical experiments were carried out in an inconel reactor to having a high purity graphite crucible, which served as an electrolyte holding vessel as well as the anode. An electropolished molybdenum rod was employed as the cathode. The electrolysis was performed at 900 °C under argon atmosphere at current densities ranging from 0.5 to 1.5 A/cm^2 at 1:6 M ratios of calcium and boron content. After the electrolysis, the cathode product was removed and cleaned using dilute HCl solution followed by triple distilled water. Characterization of the crystalline product by TG/DTA, XRD, CHNS, EDAX, XPS, EPR, and SEM were reported. From the studies, it has been observed that CaB_6 can be synthesized at all current densities and the products have some impurities.

Keywords Calcium hexaboride · Electrochemical synthesis · XRD · SEM

Introduction

Rare earth and alkaline earth metal borides belong to the group of refractory non-oxide metal-like compounds. They are characterized by a high melting point, high strength, high chemical stability, good electrical conductivity, moderate

hardness, and other special properties like low work function, stable specific resistance, low expansion coefficient in some temperature ranges, diverse magnetic orders, and high neutron absorbability. All these outstanding properties result in a wide range of applications for such material in modern equipment [1]. Calcium hexaboride (CaB_6) is a black luster crystal with low density. It is a chemically inert compound, which has a typical metal hexaboride structure, with octahedral units of six boron atoms combined with calcium (Ca) atoms. Studies have been carried out to determine the feasibility of using CaB_6 and its composites as a potential material for improvement of the abrasive resistance of bricks for convector [2, 3]. CaB_6 is used in large quantities as a deoxidizing additive for the production of magnesia carbon bricks and for the refinement of pure iron, steel, and copper [4, 5]. Furthermore, it is used as starting material for boron nitride synthesis [6]. A number of papers have been published for its production, physical, chemical, and other properties [7–12].

New investigations in the last 18 years are focused to study its electronic structure in magnetism [13]. According to Kino et al. [14] CaB_6 has a quasiparticle planed structure and semi-metallic character in bonding. Matsushita et al. [15] investigated the oxidation of CaB_6 and a composite of TiB_2 and CaB_6 . Paderno et al. [16] studied the emission characteristics of CaB_6 and $\text{CaB}_6\text{-TiB}_2$ composites. Zheng et al. [1] synthesized CaB_6 by the reaction of CaCO_3 with B_4C and carbon. Yildiz et al. synthesized CaB_6 from colemanite and petroleum coke [17]. Otani [18] prepared CaB_6 crystals by an RF-heated floating zone method. CaB_6 single crystal nanowires had been synthesized using CaO and B_2H_6 [19]. A self-catalyzed method was used for the synthesis of CaB_6 using Ca powder and BCl_3 gas mixed with H_2 and argon (Ar) [20]. However, a few papers have systematically described the synthesis of CaB_6 . The most

S. Angappan (✉) · M. Helan · A. Visuvasam · L. J. Berchmans · V. Ananth
CSIR-Central Electrochemical Research Institute,
Karaikudi 630 006, India
e-mail: angs67@gmail.com

important methods for the preparation of borides are the following.

- Synthesis of the compound through either melting pressure sintering or hydrolysis
- Reduction of the metal and boron oxide with carbon (carbothermic method)
- Reaction of the metal oxide with B_4C (B_4C method)
- Reaction of the metal and boron oxide with metals Al, Si, Mg (aluminothermic reduction, etc.)
- Molten salt method

The selection of the production method is dependent on the properties of the raw materials and the desired end product of boride. In addition, the conditions of the reaction mechanisms play a very significant role [21].

However, molten salt synthesis of CaB_6 has not been attempted. Hence, an effort has been made to synthesize this compound by the molten salt technique and the products are characterized using various characterization techniques.

Experimental

The melt used for the electrodeposition consisted of CaO (10.4 mol%), B_2O_3 (39.6 mol%), and LiF (50 mol%). All the chemicals were of analytical grade from Merck, India. Boron trioxide was prepared by melting the boric acid in inert atmosphere. The B_2O_3 acted as fluxing agent and also took part in the cell reaction. The viscosity of the melt was reduced by the addition of LiF . The electrolysis was carried out in a high-density graphite crucible (Porosity 16%, supplied by M/S Graphite India Limited) with an inner diameter of 50 mm and depth of 80 mm, which also served as the anode. The cathode was a 10-mm diameter molybdenum (Mo) rod threaded to a stainless steel rod. The graphite crucible was filled with the stoichiometric quantities of electrolytic salts, which were dried at $450\text{ }^\circ\text{C}$ under Ar atmosphere. The crucible was closed with a vacuum-tight flange with cooling arrangement and provisions for fixing electrodes, inlet/outlet for circulating Ar gas and thermocouple. The crucible was then centrally positioned and placed at the lower end of the inconel cylindrical reactor, which was kept inside a wire wound furnace with temperature control as shown in Fig. 1. The electrode could be raised or lowered through a special Teflon Swagelok seal arrangement in the flange.

Prior to the experiments, the eutectic point of the melt was determined by performing TG-DTA studies using Universal V4.3 instrument. Then, the salts were melted slowly under a continuous flow of Ar gas. The melt was equilibrated at $900\text{ }^\circ\text{C}$ for 1 h before the electrolysis. An electropolished Mo cathode was centrally positioned in the

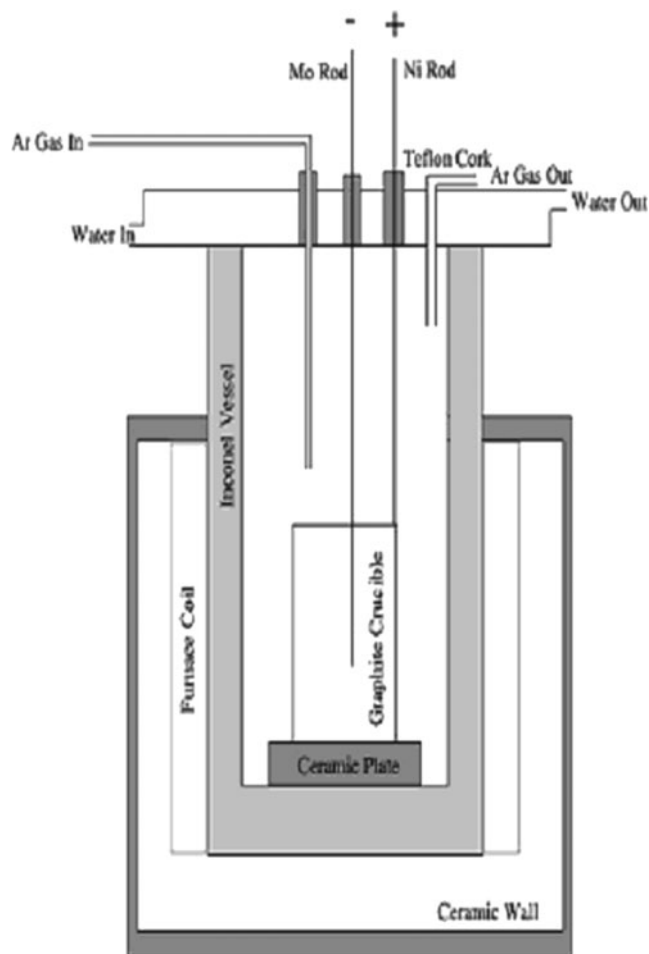


Fig. 1 Experimental set-up for the synthesis of CaB_6

melt. The bath was pre-electrolyzed at $\approx 2.0\text{ V}$ for 2 h to remove the impurities. After the pre-electrolysis, the cathode was substituted with a fresh one. Experiments were carried out at different current densities ranging from 0.5 to 1.5 A/cm^2 at 1:6 M ratios of Ca/B.

Ca and B were simultaneously reduced at the cathode to form CaB_6 , while oxygen evolved at the anode-formed oxides of carbon by reacting with the graphite anode. The variation of temperature slightly altered the potential during the electrolysis. The voltage across the cell was found to vary between 1.85 and 2.2 V. After electrolysis, the Mo cathode, enriched with the boride deposit, was raised above the melt and allowed to cool in Ar atmosphere before being taken out of the cell. The deposited boride was scraped off onto a glass plate, and the electrolyte that adhered to the boride was leached with warm 5% HCl, followed by 2% NaOH solution and then washed several times with distilled water. In all the experiments, it was observed that a good adherent deposit on the Mo cathode. The quantity of the product was found to be about 6 g. At all the current densities, the color of the final product was found to be

black. The quantity of deposit increased with the increase in current density. The average crystalline size of the deposit was found to be inversely proportional to the current density.

The phase identification of the CaB_6 powders was done using X-ray diffraction (XRD) Philips XL30W/TMP X-ray diffractometer. The morphology of the synthesized powder was scrutinized by a scanning electron microscope (SEM) (JEOL-JSM-3.5 CF, Japan). Energy dispersive X-ray spectroscopy (EDX) was performed to analyze the composition of the product using the same instrument. CHNS analysis was carried out using Elementar Vario EL III (Germany) to analyze the purity of the synthesized product. Electron paramagnetic resonance spectroscopy (EPR) was performed with a microwave frequency of 9.857403 GHz with fields corresponding to about 6,500.000 G sweep width using a Bruker Bio Spin GmbH EPR spectrometer. X-ray photoelectron spectroscopy was done to study the binding energy of boron and calcium atom using Thermo Scientific UK MultiLab 2000.

Results and discussion

The TGA/DTA curve for CaB_6 starting powder is shown in Fig. 2. From the figure, the eutectic point of the melt is found to be 820 °C. The temperature of the bath is kept

approximately 80 °C higher than the eutectic point in order to reduce the viscosity of the melt. In the electrolyte mixture, LiF is used as the supporting electrolyte because it has high electrical conductivity in its molten state. It is also more stable at high temperatures. It is more cathodic than all other salts chosen. It also provides high fluidity and decreases the eutectic temperature. A gradual loss in weight is observed up to 134 °C, due to the removal of moisture, which is also confirmed by the appearance of a single exothermic peak at 132 °C. The weight loss between the temperatures 134 °C and 737 °C is mainly due to the evaporation of B_2O_3 . The final weight loss between 833 °C and 1,000 °C is mainly responsible for the gradual transformation of the reactants into the desired product. These processes are verified by the appearance of a single exothermic peak centered at 819 °C in the DTA curve. About 28 wt.% of the weight loss occurred at 1,000 °C indicates that CaB_6 is not oxidized to conform the formation of CaB_6 [22].

The X-ray powder diffraction pattern of the CaB_6 crystal (Fig. 3) shows well-defined peaks exhibiting the presence of CaB_6 (JCPDS card no. 030662) [23]. The different bond length of the compound calculated from the XRD data is given in Table 1. The lattice constant value is determined from the XRD data, which is found to be $a=4.15 \text{ \AA}$ for CaB_6 crystals synthesized at different current densities. All peaks can be indexed with cubic lattice except for a peak at

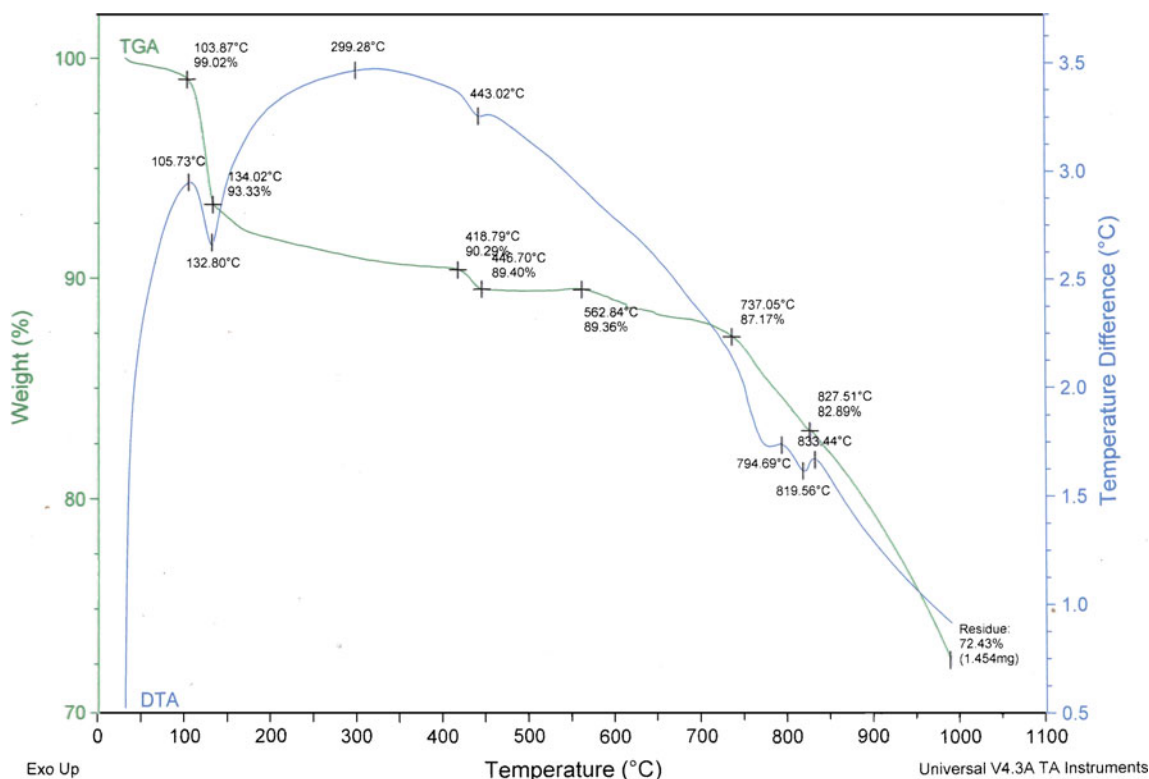


Fig. 2 TG/DTA curve for the melt $\text{CaO-B}_2\text{O}_3\text{-LiF}$

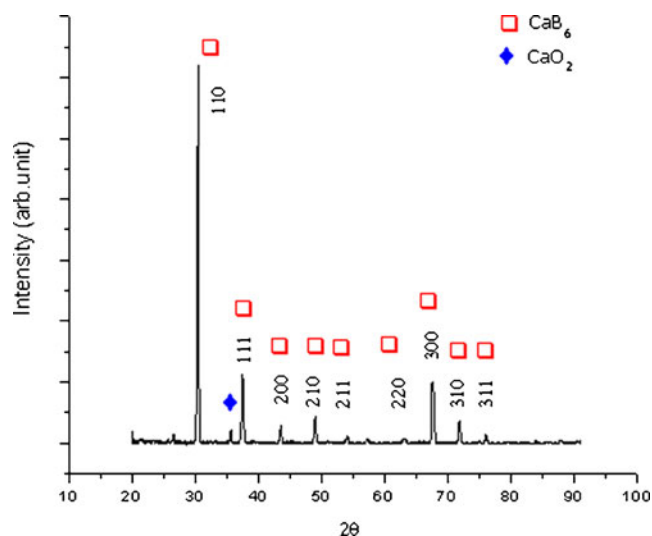


Fig. 3 XRD pattern of CaB_6 obtained at a current density of 0.75 A/cm^2

35.616 (2θ value), which corresponds to peak of CaO_2 . The reaction temperature plays an important role in determining the shape of the final product [24]. The explanation is based on the following factors that the final shape of the particles is decided by two different crystalline planes, (100) and (111), where the (111) plane has a higher surface energy than the (100) plane. Therefore, at higher temperatures the (111) plane has gained more thermal energy, which leads to the formation of most stable structure of the cubic morphology [25].

EDX analyses ascertain the purity of the compound, which is found to be more than 98%. Traces of impurities such as carbon and sulfur are identified from the CHNS analysis. The impurity level at a current density of 0.5 A/cm^2 is given in Table 2.

Figure 4 gives the XPS spectra of the synthesized CaB_6 sample. The X-ray photoelectron spectroscopy of the product CaB_6 indicates that the existence of Ca 2p, B1s, and O1s spectra are obtained. The B1s and Ca 2p core level regions are examined. It is found that the binding energy of B1s is at 191 eV and Ca 2p at 347 eV. This corresponds well with the reported binding energies for CaB_6 [26, 27]. Based on the calculation of the peak areas, the mole ratio of B/Ca is obtained to be 6.01 and close to the chemical stoichiometry of CaB_6 . Small amounts of carbon and oxygen are also detected from the XPS spectra. This suggests that the surface of the CaB_6 sample is absorbed

Table 1 Bond lengths in CaB_6 crystals at the current density of 0.5 A/cm^2

Bond	Bond length (Å)
Ca–Ca	4.15
Ca–B	3.06
B–B	1.72

Table 2 Impurities associated with CaB_6 crystals at the current density of 0.5 A/cm^2

Impurity	Weight (%)
C	0.955
S	0.277

C Carbon, S Sulphur

with oxygen and carbon due to the exposure to air during the processing of the sample.

SEM micrograph (Fig. 5) provides more details about the morphology of the products. The grain size of the crystals with homogeneous distribution of rectangular-shaped plate-like structures is found to be larger at higher current densities with prolonged holding time. The average crystalline size of the particle is ranging from 10 to 20 μm at 0.5 A/cm^2 .

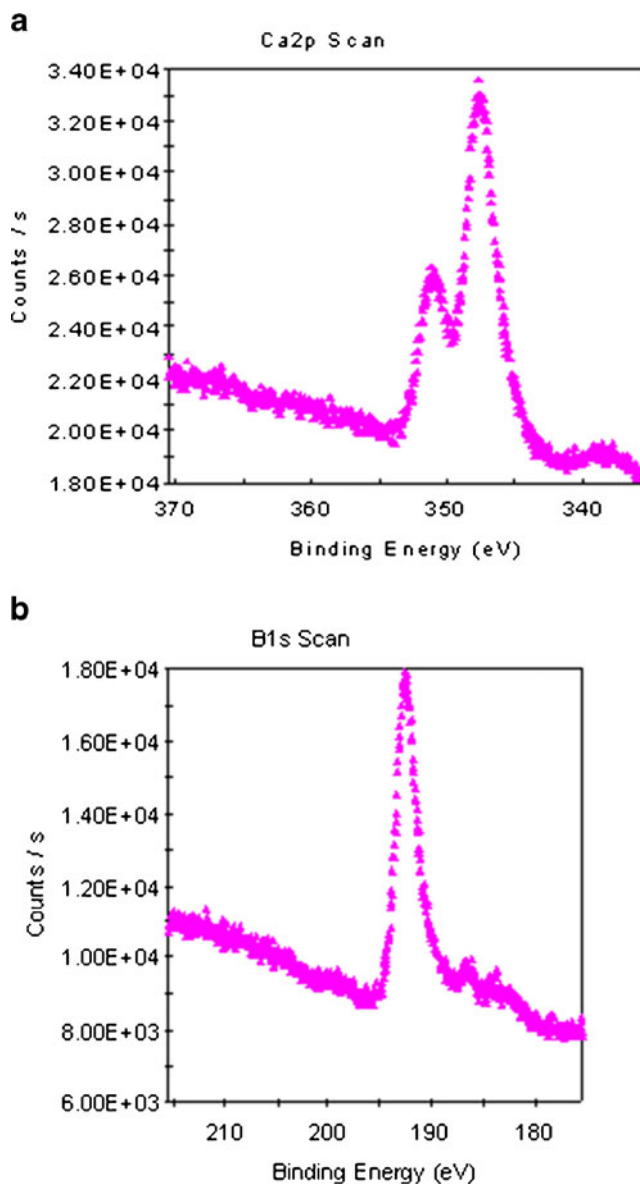
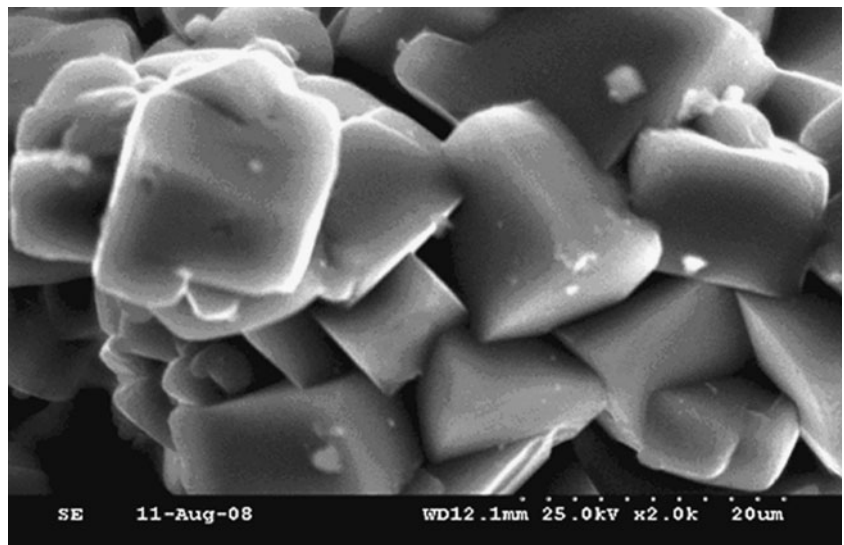


Fig. 4 XPS spectra for CaB_6 **a** Ca 2p spectrum **b** B 1s spectrum

Fig. 5 SEM images of CaB₆



EPR is a very informative and highly sensitive method of studying spin correlations in solid state. The alkaline earth hexaborides are known for their conduction through electron spin resonance. The synthesized CaB₆ crystals are

also characterized by EPR spectra (Fig. 6) at 20 °C. The g factor is found to be 2.005. The values are in good agreement with the reported value. The alkaline earth hexaborides are semiconductors that generally grow with

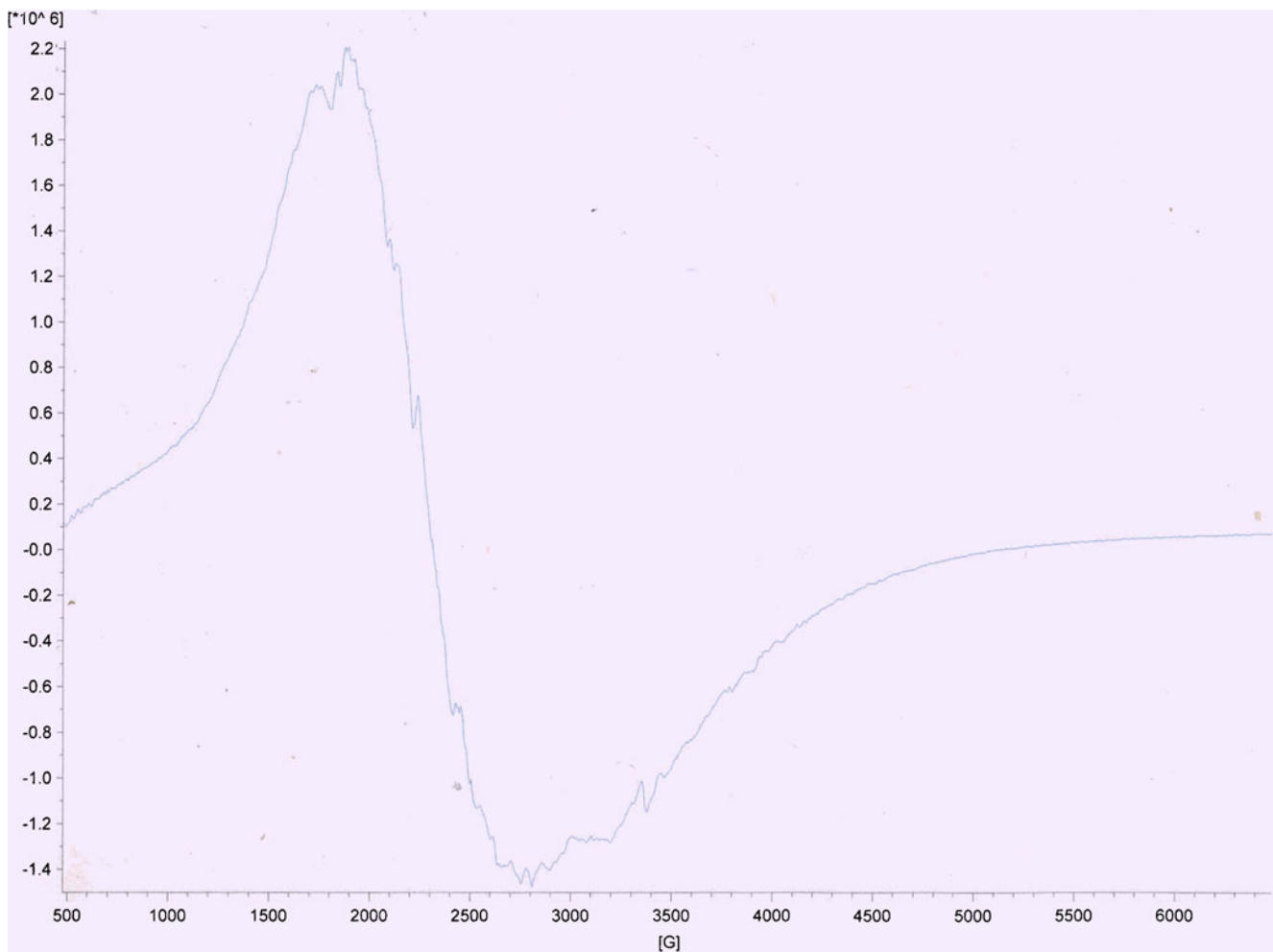


Fig. 6 EPR spectra for CaB₆

some intrinsic level of defects, most probably involving defects on the Ca and/or boron sublattice. Some of these defects can carry magnetic moment. CaB_6 is grown from a Ca-rich mixture of elements, which becomes very weakly paramagnetic, while its low temperature of less than 80 K resistivity is increased by more than two orders of magnitude [28–30].

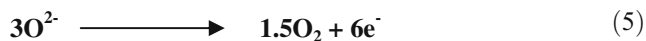
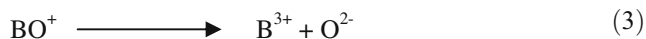
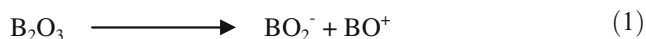
Mechanism of deposition of CaB_6

It is elucidated that both the components of the individual salts are dissolved in the ionic melt forming a thin layer of CaB_6 at electrode surface. The composition and morphology of the boride phase is being controlled by the process parameters, such as current density, cell voltage, temperature, and composition of the bath. Current density promotes the rate of deposition and influences the morphology of the ultimate product.

The presence of LiF in the electrolyte has a definite role on the deposition of this compound [31, 32]. The average grain size of the deposit decreases with increasing current density and concentration of the electrochemically active species.

Various mechanisms have been anticipated for the deposition of rare earth borides. At the outset, the dissociation of B_2O_3 takes place and gives rise to boron ions at the first instance. The commonly accepted mechanism of boron deposition in molten salts is a single-step three-electron electrochemical reaction [31–41]. The reaction mechanism can be written as follows:

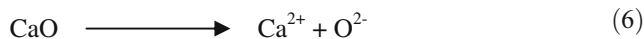
According to Uchida et al. [42] the electro decomposition of boron from B_2O_3 can be written as follows:



It is also suggested that the deposition of boron is a reversible process limited by the diffusion of boron ions

through the electrolyte [43, 44]. At the same time, the following reactions are also taking place.

The decomposition of CaO may be represented as follows:



The overall cell reaction can be written as:



The mechanism of crystal formation of hexaboride may be similar as solid state reaction at high temperatures, explained by Kalai Selvan et al. [45]. According to them, primarily, the particles of B and Ca are agglomerated, without any particular shape and are in the bath. The deposited boron on the molybdenum cathode acts as the nucleation center for the formation of hexaboride. It converts into small crystalline particles at high temperature. It is elucidated that the formation of the cubic morphology is by a thermodynamically controlled process. Finally, the fine crystalline particles are joined together to form submicron-sized crystals. Ultimately, the perfect cubic structure is obtained by electrodeposition at the cathode surface at 900 °C due to Ostwald ripening process [46]. As per the above reaction, calcium and boron are reduced at the Mo cathode to form CaB_6 . The oxygen is evolved at the anode.

Conclusion

Crystalline CaB_6 is successfully synthesized using the molten salt technique. The prepared compound possesses good physical properties. The synthesized product is found to be pure with a degree of impurity phase. The synthesis process is economically viable which can be extended for the large-scale preparation of this material.

Acknowledgements The authors express their gratitude to the director of CSIR-CECRI and staff of the EPM division for their help, and also to G.V.M. Kiruthika for her assistance in the XPS measurements.

References

- Zheng S, Min G, Zou Z, Yu H, Han J (2001) *J Am Ceram Soc* 84:2725

2. Hanagiri S, Harada T, Aso S, Fujiwara S, Yasui H, Takanaga S, Takahashi H, Watanabe A (1992) *Taikabutu* 44:490
3. Hanagiri S, Fujiwara S, Kasahara H, Umehara I, Yasui H, Nonobe K, Takahashi H (1992) *Taikabutu* 44:640
4. Rymon-Lipinski T, Schmelzer B, Ulitzka S (1994) *Steel res* 65:234
5. Hunold K (1995) *Ceram Int* 144:47
6. Schwetz KA, Lipp A (1979) *Ber Dt Keram Ges* 56:1
7. Schwetz KA, Reinmuth K, Lipp A (1981) *Redex Rundschau* 3:568
8. Blumm P, Bertaut F (1954) *Acta Crystallogr* 7:81
9. Vekshina NV, Markovskii LY (1962) *J Appl Chem* 35:23
10. Markovskii LY, Vekshina VN (1958) *J Appl Chem* 31:1280
11. Samsonov GV, Paderno Yu B, Fomenko S (1963) *Soviet Powder Metall* 6:449
12. Greenwood NN, Parish RV, Tornton P (1965) *J Chem Soc* 168:545
13. Tromp HJ, Van Gelderen P, Kelly PJ, Brocks G, Bobbert PA (2001) *Phys Rev Lett* 87:016401(R)
14. Kino H, Aryasetiawan F, Terakura K (2002) *Phys Rev B* 66:121103(R)
15. Matsushita J, Mori K, Sawada Y (1998) *J Mater Synth Process* 6:407
16. Paderno VN, Paderno YB, Martynenko AN, Volkogon VM (1992) *Porosk metall* 10:52
17. Yildiz O, Telle R, Schmalzried C, Kaiser A (2005) *J Eur Ceram Soc* 25:3375
18. Otani S (1998) *J Cryst Growth* 192:346
19. Xu TT, Zheng JG, Nicholls AW, Stankovich S, Piner RD, Ruoff RS (2004) *Nano Lett* 4:2051
20. Xu J, Zhao Y, Zou C, Ding Q (2007) *J Solid State Chem* 180:2577
21. Etourneau J, Mercurio J-P, Hagenmuller P (1977) Boron and refractory borides, In: Matkovitch VI (ed). Berlin, Heidelberg, New York, Springer, pp 115
22. Zheng SQ, Min GH, Zou ZD, Tatauyama C (2004) *Mater Lett* 58:2586
23. Song M, Yang IS, Kim JY, Cho BK (2006) *Vib Spectrosc* 42:288
24. Lee SM, Cho SN, Cheon J (2003) *Adv Mater* 15:441
25. Jose TP, Sundar L, Berchmans LJ, Visuvasam A, Angappan S (2009) *J Min Metall* 45:101
26. Sekiyama A, Sasabayashi T, Higashiya A, Fujiwara H, Imada S, Taniguchi K, Takagi H, Katsufuji T, Kitazawa K, Suga S (2005) *J Electron Spectros* 659:144–147
27. Shi L, Gu Y, Qian T, Li X, Chen L, Yang Z, Ma J, Qian Y (2004) *Phys C* 405:271
28. Rupp LW, Schmidt PH (1969) *J Phys Chem Solids* 30:1059
29. Fisk S, Ott HR, Barzykin V, Gorkov LP (2002) *Phys B* 312–313:808
30. Ott HR, Chernikov M, Felder E, Degiorgi L, Moshopoulou EG, Srrao JL (1997) *Z Phys B* 102:337
31. Thompson R (1970) *Prog Boron Chem* 2:173
32. Lipscomb WN (1981) *J less-common Met* 82:1
33. Davis PR, Gesley MA, Schwind GA, Swanson LW (1989) *Appl Surf Sci* 381:37
34. Meschel SV, Kleppa OJ (1995) *J alloys compd* 226:243
35. Bala Krishnan G, Lees MR, McK D, Daul (2003) *J Cryst Growth* 256:206
36. Zou CY, Zhao YM, Xu JQ (2006) *J Cryst Growth* 291:112
37. Ka T, Bannai E, Kawai S, Yamane T (1975) *J Cryst Growth* 30:193
38. Greenwood NN, Earnshaw A (1997) *Chemistry of the elements*. Reed Educational and Professional Publishing Ltd., UK, pp 139
39. Etourneau J, Hagen Muller P (1985) *Philos Mag* 52:589
40. Duncan RN, Arney TL (1984) *Plat Surf Finish* 49:49
41. Goldie W (1968) *Metallic coating of plastics*. Vol I, Electrochemical Publications Ltd., Middlesex, UK
42. Uchida K (1978) *Sur Technol* 7:137
43. Taranenko V, Zarutskii IV, Shapoval VI, Makyta M, Matiaovský K (1992) *Electrochim Acta* 37:263
44. Zarutskiy IV, Malishev VV, Shapoval VI (1997) *Zh Prikl Khim* 70:1475
45. Kalai Selvan R, Genish I, Perelshtein I, Jose M (2008) *J Phys Chem C* 112:1795
46. Zeng J, Wang H, Zhang Y, Zhu MK, Yan H (2007) *J Phys Chem C* 111:11879